Automotive interior cabin noise analysis and optimization using Statistical Energy Analysis and Response Surface Methodology

Javad Marzbanrad[1*], Mohammad Hafezian, Mehdi Mozaffarikhah

Associate Professor, School of Automotive Engineering, Iran University of Science and Technology

ARTICLE INFO	A B S T R A C T
	In this paper, the acoustic analysis of noise has been done in automotive cabin at high speed. High-frequency noise sources are applied separately to the roof and floor panels as well as to the windshield of the vehicle, which has been investigated at both the driver's and rear passenger's head. The most important panels that have the most noise emission are specified. In order to analyze high frequencies, the Statistical Energy Analysis (SEA) method has been used; also, the Response Surface Methodology (RSM) has been used to obtain optimized panel in terms of minimally weighing and maximum noise reduction. The results show that the proposed panels with unconstrained rubber layer can reduce the cabin interior aerodynamically generated noise more than %6.

1. Introduction

Reduction of interior noise and vibration in vehicles is an important factor in accomplishing world-class vehicle. Automotive interior noise is usually the mixture of noises arisen from different sources such as engine, power train, climate control systems and road inputs, which is transferred through different paths [1], [2]. Because of improvement in engine noise and power transmission noise, nowadays, one of the main interior noises in automotive comes from aerodynamic noise in high both speeds and frequencies. In high speeds, much interior noise is caused by transmission of external pressure fluctuations through windows and other surfaces. Buchheim [3] showed that the most important source of noise is aerodynamic noise in 100 mph velocity.

Experimental noise control process is costly and time-consuming. It is well known that numerical methods, due to their high speed and accuracy are very common methods for testing noise control.

In this paper, considering the limited frequency in finite element analysis (FEA) and boundary element analysis (BEA), the statistical energy analysis (SEA) method is used. Statistical energy analysis (SEA) can predict sound and vibration levels through large complex systems at mid and high frequencies [4]. Finite element and boundary element methods accurately predict vibro-acoustic in the low- to mid-frequency range from 20 Hz to 500 Hz [5]. However, SEA can predict the airborne noise inputs noise in the range more than 500 Hz accurately as mentioned by Remington and Manning [6]. Radcliffe and Huang [7] presented a methodology for extending the design application of the SEA method to predict the response of vibro-acoustic automotive structure and interior space. Kook and Colleagues [8] measured interior noise level based on a simple power law which the mean squared acoustic pressure was used for the interior noise determination. Putra et al [9] used substitution source method to measure the airborne noise in a car cabin and showed that the transition frequency

*Corresponding Author
Email Address: marzban@iust.ac.ir
10.22068/ijae.9.1.2887

is independent of the engine speed. Nopiah et al [10] studied the impacts of vibration on noise in a vehicle cabin and used a goal programming model to optimize the noise annoyance level in the cabin. The vibration caused by the interaction between the tire and road surface, as well as the effects of noise caused by it in a car cabin was investigated by Nopiah et al. [11]. Finally, they presented a method for predicting these effects. Kurosawa [12] measured airborne noise by Hybrid Statistical Energy Analysis (HSEA) in order to decrease noise level and also weight of acoustic insulations. Shell and Cotoni [13] combined FE and SEA model to in order to perform an aero-vibro-acoustic analysis of a Mercedes-Benz A-class.

Viscoelastic materials for automobile body, floor and dash panels have been undergoing rapid advancements in recent years. Expectations regarding viscoelastic materials are also increasing since the requirement of preferable interior sound quality and weight reduction has increased. Viscoelastic damping material improve the vibration insulation which will reduce the noise component [14], [15]. Inactive noise control is widely used on account of the active way's cost and complexity. In case of free viscoelastic layers shown in Figure 1, the shear strain and the dilatation in the viscoelastic layer are of the same order as introduced by Ross and Kerwin [16]. They conducted the vibration analysis of a plate with a viscoelastic layer. Rao [1] showed that significant noise reduction can be achieved in low frequencies by additive damping treatment. Lee [17] investigated the noise reduction of panels with free layer viscoelastic materials.

In this study, the formulation of turbulent boundary layer loads is expressed first. Then, a simple 3D model of the vehicle was considered and Sound Pressure Level (SPL) without any noise control treatment (NCT) for major excitations in different locations was calculated. The three crucial areas of body of the vehicle which have the most influence on aerodynamically generated noise have been diagnosed. As noise control treatment (NCT), steel panel with unconstrained layer of rubber on the roof panel was used to reduce the interior cabin noise. An ubiquitous type of material used in the present applications is based on ''Nitrile'' type rubber as introduced by Alvelid and Enelund [18]. The RSM approach was used to investigate the possible effects of steel and rubber thickness on the noise reduction. Finally, the optimized panel in aspects of noise reduction considering panel weight was proposed and its effect on noise

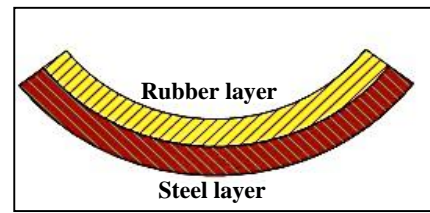reduction in automotive interior cabin has been investigated.

Figure 1: Configuration of steel plate with unconstrained layer of rubber

2. Turbulent boundary layer load

Turbulent pressure is used to model a boundary layer flow excitation over the surface area of a plate or shell subsystem. Figure 2 shows the turbulent boundary layer over two subsystems. The function of root-mean-square pressure provides an average pressure because it is not possible to merely use the mean pressure of a wave form. The rms pressure is most often used to describe a sound wave because it is related to the energy, which is called the intensity. Therefor the intensity depends on the average of the pressure squared thus the average must be used. Histograms of the pressure fluctuations, p_{rms}/q, is true for all cases of continuous sound time histories including noise and pure tones. Dynamic pressure loads have two important characteristics:

a)   A band-integrated root-mean-square (rms) pressure spectrum.

b)   A narrowband Spatial Correlation Function (SCF) between the pressure variations at any two points on the loaded surface.
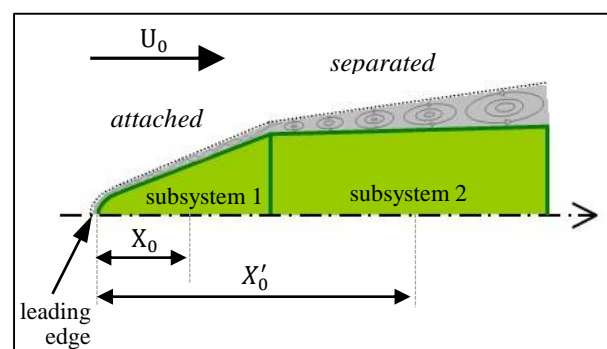

Figure 2: Turbulent boundary layer over two subsystems

The rms pressure defines as following equation:

$$\frac{p_{rms}}{q} = \begin{cases} \frac{0.006}{1+0.14M^2} & if\ attached \\ \min(0.026 + \frac{0.041}{1+1.606M^2}) & if\ seperated \end{cases} \quad (1)$$

$$q = \frac{1}{2}\rho U_0^2, \ \ M = \frac{U_0}{c_0} \quad (2)$$

where p_{rms} is rms pressure spectrum, ρ is fluid density, U_0 is free stream flow velocity and c_0 is fluid speed of sound.

The narrowband spatial correlation function R takes the following normalized form:

$$R\langle\bar{x}|\bar{x},w\rangle = exp\big(-c_x\,|x'-x|/d - c_y\,|y'-y|/d\big) \times \cos(k_x(x'-x)) \times \cos\big(k_y(y'-y)\big)\big) \quad (3)$$

$$1/d = \sqrt{k_x^2 + k_y^2 + \frac{1}{9\delta_*^2}}, \quad \delta_* = \frac{\delta}{8}, \quad \delta = 0.37\frac{X_0}{Re^{1/5}} \quad or \quad \delta = 0.37\frac{X_0'}{Re^{1/5}} \quad (4)$$

where, X_0 and X_0' are the distance from the leading edge of the turbulent boundary layer to the center of pressure load on the surface of the subsystems, d is the thickness of the boundary layer, Re is the Reynolds number, and $\{k_x, k_y\}$ are the components of the wave vector of the flow with regard to the X-Y coordinate axes of the plate/shell [19], [20].

In turn k_x and k_y are defined as fractions of the characteristic wavenumber $k_c = w/U_c$, where U_c is the flow convection velocity of the turbulence.

The dimensionless parameters c_x and c_y in the exponentially decaying part of the spatial correlation function are the spatial correlation coefficients of decay in the X and Y direction respectively. For instance, if the direction of the turbulence flow is parallel to the X-axis of the plate /shell, then typical values are: $c_x = 0.1, c_y = 0.72$ as mentioned by Rennison and colleagues [19]. If the direction of the turbulence flow is parallel to the Y-axis of the plate/shell, then those typical values become: $c_x = 0.72, c_y = 0.1$

When the dynamic pressure loads have been calculated, the SEA power balance between outer cavity (turbulent boundary layer), plate/shell and interior cavity results the sound pressure level (SPL) in the interior cavity.

The sound pressure level L_p is given by

$$L_p = 10\log_{10}\left(\frac{(p^2)_t}{P_{ref}^2}\right) = 10\log_{10}\left(\frac{p_{rms}^2}{P_{ref}^2}\right) = 20\log_{10}\left(\frac{p_{rms}}{P_{ref}}\right) dB \quad (5)$$

where P_{ref} is the reference pressure, $P_{ref} = 20\,\mu$Pa $= 0.00002\,N/m^2$ for air [21].

3. Validation

John and Wang [22] studied acoustic transfer function test in a passenger vehicle. The vehicle was equipped by an external exciter which is a loudspeaker; as well as that two microphones were used to measure the performance of the power train noise transfer function in the car; one

in the driver's head near the loudspeaker, and the other on the right side of the engine compartment near the firewall. In order to gather and process data, microphones were connected to a computer through preamplifiers. Eventually, the data were analyzed using FFT analysis. The same AutoSEA vehicle simulation model and material model were established here. The power train acoustic transfer function was calculated. The simulation and analysis results are shown in Figure 3. It shows that simulated and measured power train noise (which is created with the diffuse field excitation source) acoustic transfer functions match quit well with each other between 700 and 3000 Hz.
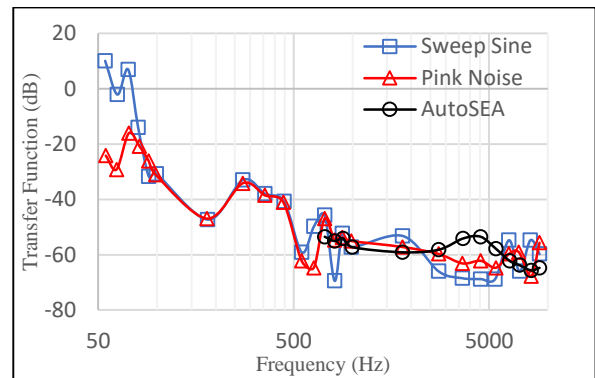

Figure 3: Acoustic transfer function

4. Modeling and Simulation

Figure 4 shows the 3D model of the vehicle in AutoSEA. The vehicle structure was divided into plates/shells and acoustic subsystems. Plate/shell subsystems were used to represent the floor, dash, roof, windows, doors and firewall as stated in Table 1. The interior was subdivided into acoustic spaces which they are classified into front driver's head cavity and rear passenger's head cavity as illustrated in Figure 5.
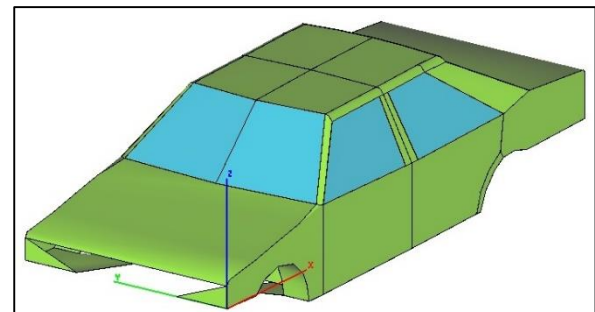

Figure 4: Automotive body 3D model

Table 1: Automotive panels properties

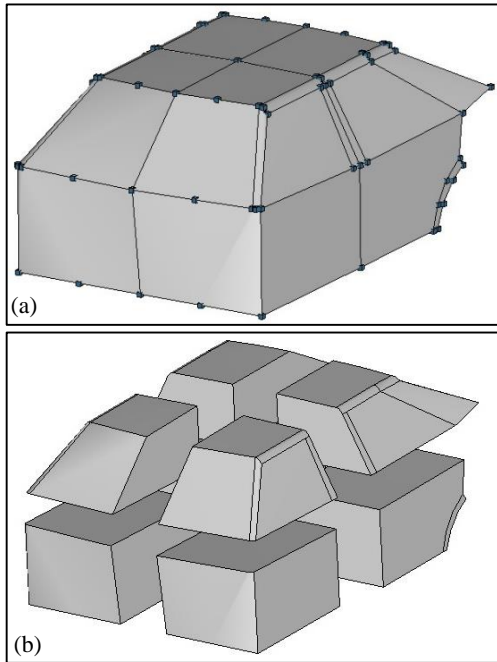| Structure	Type of Material	Thickness (mm)
Floor panel	Steel	0.8
Roof panel	Steel	0.8
Door panels	Steel	0.8
Seat shells	Foam	100
Pillars	Steel	1.2
Glass panels	Glass	2.8

Figure 5: (a) Entire cavity, (b) Driver's and passenger's head cavity (Shrink mode)

5. Discussion

There are few types of excitation that were simulated. Turbulent boundary layer with 90 km/h free stream flow velocity is used here where roof panel, side door panels, a pillar, windscreen panels and floor panels excited separately. Finally, the SPL of driver's head cavity and rear passenger's head cavity was calculated. Then SPL of cavities when all excitations are applied has been determined and shown in Figure 6 and 7.
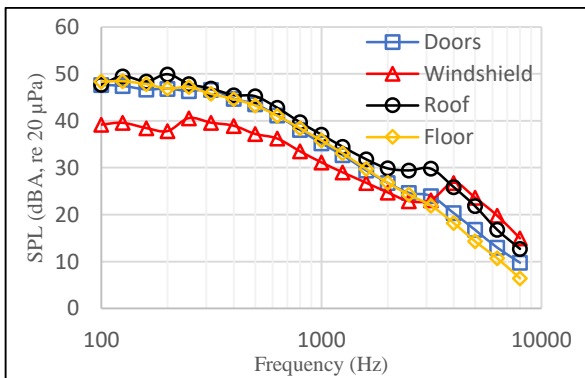

Figure 6: Interior Noise Level. Driver's head cavity for automotive parts excitations
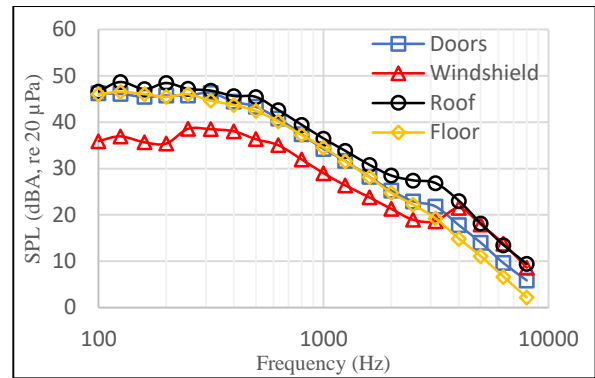(1/3 Octave band, A-weighted)

Figure 7: Interior Noise Level. Rear passenger's head cavity for automotive parts excitations
(1/3 Octave band, A-weighted)

Figure 6 and 7 show sound pressure level (SPL) overall at the driver's head and rear passenger's head, respectively. In the case of the noise response at the front seat position, the roof and doors are consistently the first and second main contributors. The roof, windscreen and side doors are the top three contributors for the rear passenger.

According to Figure 8, the driver at all range of frequencies feels more level of SPL than rear passengers when all excitations including windscreen, roof and side doors were stimulated. This SPL difference increases with enhancement of frequency. Accordingly, the most aim of noise control must be focus on noise reduction in the driver position. By controlling driver position sound level, the noise of rear passenger automatically would be controlled.
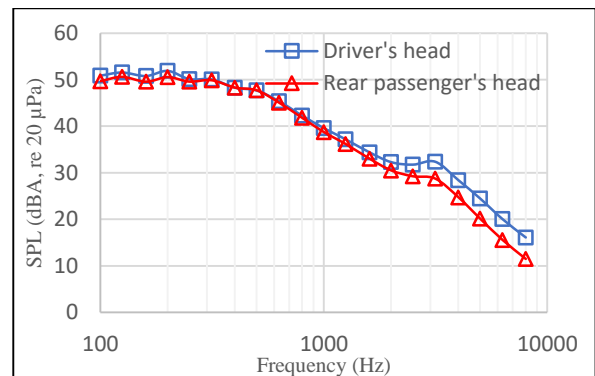

Figure 8: SPL of driver's and rear passenger's head with all parts excitation
(1/3 Octave band, A-weighted)

6. Noise Control Treatment (NCT)

Some automotive body panels have more effect on radiation aerodynamically generated noise in interior cabin. Therefore, from the perspective of noise control treatment (NCT), these panels should be considered more attention. In this paper,

the Autosea lay-up noise control treatment (NCT) for roof was considered.

Steel and Aluminum panels are widely used in automotive roof, doors and floor. LD–400 and ISD–110 are among most common viscoelastic materials which are used in automotive industry as noise and vibration reducers. Foams are applied as noise isolator as well. Alvelid and Enelund [18] investigated the damping characteristics of constrained thin layer of "Nitrile" type rubber. In this step, steel and aluminum panels coated with LD–400, ISD–110, foam and nitrile, which materials properties have been presented in Table 2, have been assumed and the best panel in term of aerodynamic noise reduction has been obtained.

Table 2: Mechanical properties of LD–400, ISD–110, foam and nitrile rubber

Material	Young's Modules (GPa)	Density (kg/m^3)	Poisson's ratio ()
LD–400	1.52	1524	0.3
ISD–110	1.796	968	0.38
Foam	0.095	40	0.3399
Nitrile	2.3	1000	0.4993

Figure 9 shows SPL in the driver's head cavity with just roof excitation when steel and aluminum roof panel with thickness of 0.8 and 1.4 mm, respectively, coated with 0.6 mm thickness of ISD–110. As can be illustrated in this figure, the SPL has been decreased.
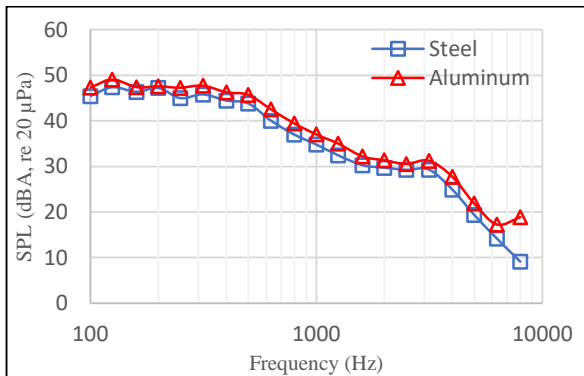

Figure 9: Effect of steel and aluminum in the roof with roof stimulation
(1/3 Octave band, A-weighted)

Figure 10 shows the effect of damping materials on aerodynamics noise reduction. For this reason, roof steel panel with thickness of 0.8 mm with 0.6 unconstrained layers of LD–400, ISD–110, foam and nitrile was assumed and SPL in the driver's head cavity has been calculated. The Average of damping materials effect on driver's head have been presented in Table 3.
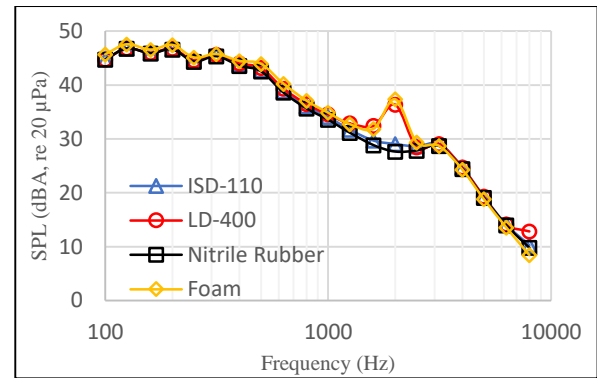

Figure 10: Damping materials effect on driver's head cavity noise reduction with roof excitation
(1/3 Octave band, A-weighted)

Table 3: Average of damping materials effect on driver's head

Damping materials	SPL
ISD-110	34.33
LD-400	35.11
Nitrile rubber	33.94
Foam	35.18

According to Figure 9 and 10 and Table 3, the steel and nitrile type of rubber have better response to aerodynamically generated noise reduction. Therefore, steel panel containing unconstrained layer of rubber was used as NCT. For optimization, the roof steel panel with thickness of 0.6 to 0.9 mm and rubber with thickness of 0.1 mm to 0.6 mm were assumed; and the effect of roof panel on noise reduction in driver position has been compared.

7. Response Surface Methodology (RSM)

To select the optimized panels in term of noise reduction and weight, the Response Surface Method (RSM) optimization has been used. The desirable outputs are panels with both maximum noise reduction and minimum weight.

Full first-order and second-order polynomial model has been fitted to the obtained data and the coefficients of the model equation have been determined by Baş and Boyacı [23] as stated in equations below:

$$y_i = \beta_0 + \beta_1 x_{i1} + \beta_2 x_{i2} + \cdots + \beta_q x_{iq} + \varepsilon_i \quad i = (1, 2, \ldots, N) \tag{6}$$

$$y = \beta_0 + \sum_{j=1}^{q} \beta_j x_j + \sum_{i=1}^{q} \beta_{jj} x_j^2 + \sum \sum_{i<j} \beta_{ij} x_i x_j + \varepsilon \tag{7}$$

where $\beta_0, \beta_i, \beta_{ii}$ and β_{ij} are regression coefficients for the intercept, linear, quadratic and interaction coefficients, respectively, X_i and X_j are the coded independent variables.

To optimize panel thickness in term of noise reduction, SPL reduction has been assumed. In

other word, difference between SPL of driver's head cavity for original case (uniform plate) and optimized case (steel panel with unconstrained rubber layer) should be compared. Table 4 shows Optimized unconstrained panels with minimum weight.

Table 4: Optimized unconstrained panels with minimum weight

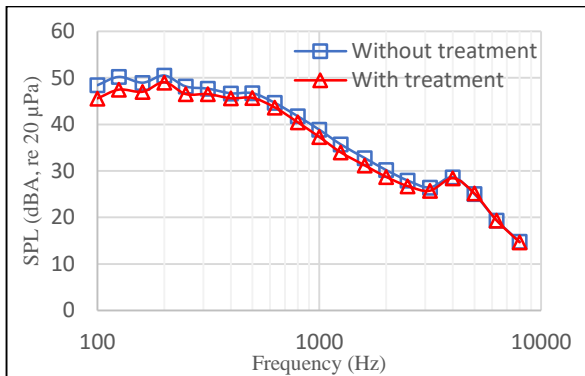| Panels	Steel Thickness (mm)	Rubber Thickness (mm)
Roof	0.7242	0.6
Floor	0.7121	0.6

Figure 11: SPL in driver's head cavity before and after treatment
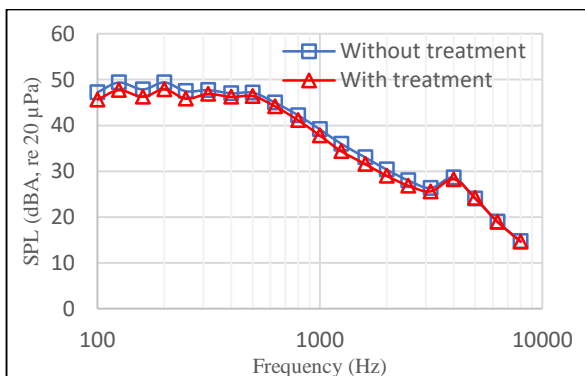(1/3 Octave band, A-weighted)

Figure 12: SPL in rear passenger's head cavity before and after treatment
(1/3 Octave band, A-weighted)

From Figure 11 and 12, it can be deduced that if steel panels with unconstrained layer of rubber be used in roof, the improvement in aerodynamic noise reduction can be observed. The values of noise reduction at driver's and rear passenger's head are 1.75 dB and 1.3 dB respectively. Furthermore, Figure 13 and 14 shows the disparity between interior noise level and illustrate that treatment floor panels with unconstrained layer of rubber can reduce aerodynamic noise level. The noise reduction values at driver's and rear passenger's head are 2.12 dB and 1.75 dB respectively.
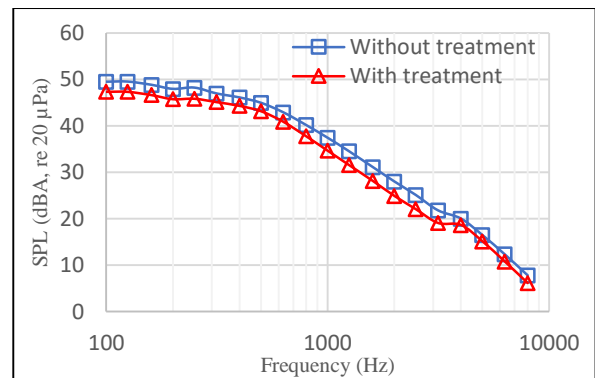

Figure 13: Driver's head cavity for common and optimized floor panel
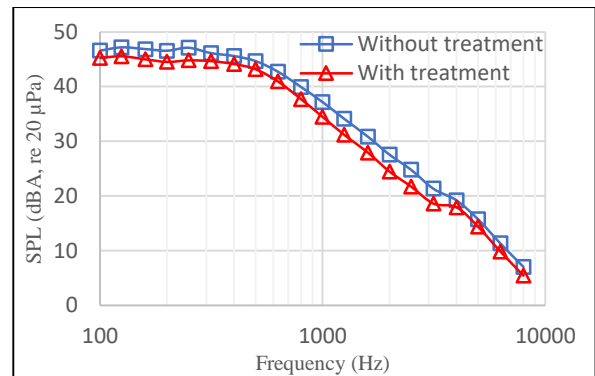(1/3 Octave band, A-weighted)

Figure 14: Rear passenger's head cavity for common and optimized floor panel
(1/3 Octave band, A-weighted)

Using free layer of rubber in the roof and floor more than %6 cabin aerodynamically generated noise would be reduced. As a result, in term of cost and noise reduction, using steel panels with unconstrained layer of rubber in roof and floor is more cost-efficient for auto-makers.

Three different kind of laminated glass (Soda-lime-silica glass) are used as windshield in vehicle modeled in AutoSEA. Polyvinyl butyral (PVB) and SentryGlas Plus (SGP), which is five times stronger than PVB material, have been proposed as interlayers for laminated glass [24]. Moreover, a bi-layer windshield including one outer ply of glass and one ply of polyurethane has been used. The result of using optimized laminated glass, as shown in Figure 15 and 16, clearly demonstrate that PVB and SGP are the most effective material in noise decline. Based on the obtained values, the amounts of noise reduction using PVB and SGP as interlayers at driver's head are 5.75 and 5.67 and at rear passenger's head are 6.5 and 6.4 respectively. The optimized values of laminated glass with minimum weight are shown in Table 5.

Table 5: Optimized laminated glass with minimum weight

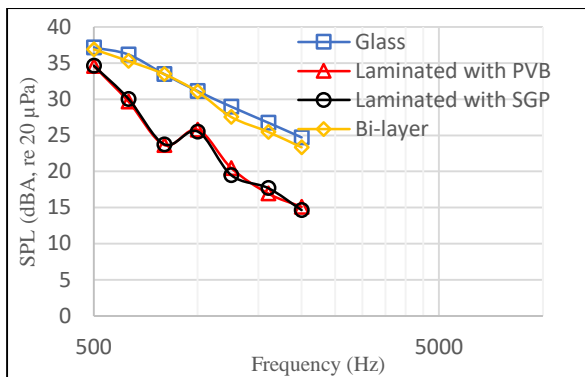| Laminated glass with PVB/SGP	Glass (mm)	Interlayer (mm)
PVB	2.18	1.5
SGP	2.2	1.5

Figure 15: Disparity in different glass material for front windshield
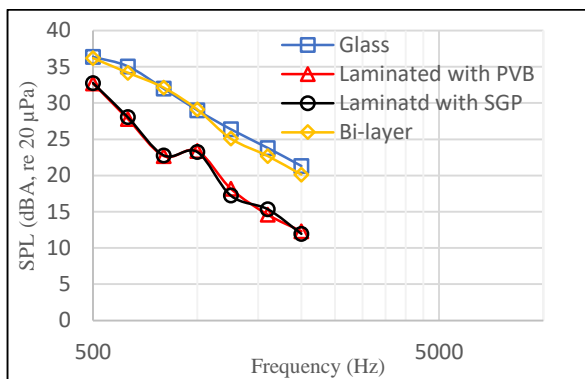(Driver's head, 1/3 Octave band, A-weighted)

Figure 16: Disparity in different glass material for front windshield
(Rear passenger's head, 1/3 Octave band, A-weighted)

The value of reducing noise pressure in cabin by using optimized treatment panels for roof and floor and also laminated glass as front windshield is shown in Table 6.

Table 6: Aerodynamic noise reduction

Optimized panels	Driver's head (dB)	Rear passenger's head (dB)
Roof	1.75	1.3
Floor	2.12	1.75
Laminated glass (PVB)	5.75	6.5
Laminated glass (SGP)	5.67	6.4

8. Conclusion

The aim of this research was an investigation of aerodynamic noise reduction in automotive interior cabin using steel panel containing thin layer of viscoelastic materials (Rubber). AutoSEA software was used for simulations in different conditions. Vehicle 3D model was created and exterior excitations have been set on automotive plates and shells. The Sound Pressure Level (SPL) as noise criteria in automotive interior cabin in different areas was calculated. The speed of free stream flow is considered 90 Km/h as exterior aerodynamic excitation. For noise reduction comparison, steel panel with thin unconstrained layer of rubber with different thickness was employed. Furthermore, as shown above laminated glass with PVB and SGP interlayer are identical in noise reduction but SGP has already been pointed above is stronger and lighter. Therefore, SGP can provide more safety for the driver and passengers in addition to reducing the noise. The Response Surface Methodology (RSM) was used to assess the optimal panel properties. The desirable panel is the one which has the most noise reduction while has minimum weight. The result of calculation shows that the optimal panel can reduce more than 6% of aerodynamic noise in the automotive cabin.

References

[1] M. D. Rao, Recent applications of viscoelastic damping for noise control in automobiles and commercial airplanes. Journal of Sound and Vibration, Vol.262, No.3, (2003), pp.457-474.

[2] X. L. Qin, X. X. Jin, Q. Zhang, P. Cheng, F. Sun, Analysis of mid-frequency vehicle structure noise with FE-SEA hybrid method. In Electric Information and Control Engineering (ICEICE), 2011 International Conference on (pp. 2002-2006). IEEE, 2011.

[3] R. Buchheim, W. Dobrzynski, H. Mankau, D. Schwabe, Vehicle interior noise related to external aerodynamics. International Journal of Vehicle Design, Vol.3, No.4, (1982), pp.398-410.

[4] S. A. Hambric, S. H. Sung, D. J. Nefske, (Eds.), Engineering vibroacoustic analysis: methods and applications. John Wiley & Sons, (2016).

[5] R. Citarella, L. Federico, A. Cicatiello, Modal acoustic transfer vector approach in a FEM–BEM vibro-acoustic analysis. Engineering Analysis with Boundary Elements, Vol.31, No.3, (2007), pp.248-258.

[6] P. J. Remington, J. E. Manning, Comparison of Statistical Energy Analysis power flow predictions with an "exact" calculation. The

Journal of the Acoustical Society of America, Vol.57, No.2, (1975), pp.374-379.

[7] C. J. Radcliffe, X. L. Huang, Putting statistics into the statistical energy analysis of automotive vehicles. Journal of Vibration and Acoustics, Vol.119, No.4, (1997), pp.629-634.

[8] H. S. Kook, D. Lee, K. D. Ih, Vehicle interior noise model based on a power law. International Journal of Automotive Technology, Vol.12, No.5, (2011), pp.777.

[9] A. Putra, F. A. Munir, C. D. Juis, On a simple technique to measure the airborne noise in a car interior using substitution source. International Journal of Vehicle Noise and Vibration, Vol.8, No.3, (2012), pp.275-287.

[10] Z. M. Nopiah, A. K. Junoh, A. K. Ariffin, Optimisation of acoustical comfort in vehicle cabin using goal programming. International Journal of Vehicle Noise and Vibration, Vol.9, No.3-4, (2013), pp.194-215.

[11] Z. M. Nopiah, A. K. Junoh, A. K. Ariffin, Computational method for predicting the effects of vibrations to acoustical comfort in vehicle cabin. International Journal of Vehicle Noise and Vibration, Vol.10, No.1-2, (2014), pp.150-170.

[12] Y. Kurosawa, Predicting Automotive Interior Noise Including Wind Noise by Statistical Energy Analysis. World Academy of Science, Engineering and Technology, International Science Index 111, International Journal of Mechanical, Aerospace, Industrial, Mechatronic and Manufacturing Engineering, Vol.10, No.3, (2016), pp.635 - 641.

[13] A. Schell, V. Cotoni, Flow induced interior noise prediction of a passenger car. In INTER-NOISE and NOISE-CON Congress and Conference Proceedings, Institute of Noise Control Engineering, Vol.254, No.2, pp.1-10, November 2017.

[14] M. D. Rao, Recent Applications of Viscoelastic Damping in Automobiles and Commercial Airplanes, India-USA Symposium on Emerging Trends in Vibration and Noise Engineering, 2001.

[15] X. Q. Zhou, D. Y. Yu, X. Y. Shao, S. Q. Zhang, S. Wang, Research and applications of viscoelastic vibration damping materials: a review. Composite Structures, Vol.136, (2016), pp.460-480.

[16] D. Ross, E. M. Kerwin, E. E. Ungar, Damping of Plate Flexural Vibration by Means of Viscoelastic Laminate. Structural Damping, ASME, New York, (1959).

[17] D. H. Lee, W. S. Hwang, Layout optimization of unconstrained viscoelastic layer on beams using fractional derivative model. AIAA journal, Vol.42, No.10, (2004), pp.2167-2170.

[18] M. Alvelid, M. Enelund, Modelling of constrained thin rubber layer with emphasis on damping. Journal of Sound and Vibration, Vol.300, No.3-5, (2007), pp.662-675.

[19] D. Rennison, A. G. Piersol, J. F. Wilby, E. G. Wilby, A review of the acoustic and aerodynamic loads and the vibration response of the Space Shuttle Orbiter vehicle–STS-1 dynamics verification assessment. Bolt Beranek and Newman Report 4438 for NASA, Jet Propulsion Laboratory. (1980).

[20] M. Baker, C. Pray, Understanding Critical Dynamic Loads for Nozzle and Nozzle Extension Design. In 47th AIAA/ASME/SAE/ASEE Joint Propulsion Conference & Exhibition, (2011), p. 5686.

[21] M. J. Crocker, Handbook of Noise and Vibration Control, John Wiley & Sons, 2007.

[22] T. K. John, X. Wang, Vehicle floor carpet acoustic optimisation using statistical energy analysis. International Journal of Vehicle Noise and Vibration, Vol.5, No.1-2, (2009), pp.141-157.

[23] D. Baş, I. H. Boyacı, Modeling and optimization I: Usability of response surface methodology. Journal of food engineering, Vol.78, No.3, (2007), pp.836-845.

[24] X. Zhang, Y. Shi, H. Hao, J. Cui, The mechanical properties of ionoplast interlayer material at high strain rates. Materials & Design, Vol.83, (2015), pp.387-39.